Duality in the Topological Holography Framework

Xie Chen

July 20, 2024

1 Introduction

Duality is a useful idea used in many different contexts. In quantum physics, there is particle-wave duality, electric-magnetic duality of electromagnetism, boson-vortex duality of 2+1D boson system, Kramers-Wannier duality of 1+1D Ising model, and AdS-CFT correspondence of quantum gravity. In cases like electric-magnetic duality, boson-vortex duality, and AdS-CFT, dual theories provide different descriptions of the same underlying physics. This can be useful especially if one of the theories is weakly interacting and hence easy to do calculations with while the other theory may be strongly interacting and hard to compute any quantity. Examples like Kramers-Wannier are self-dualities that map a theory back to itself but with a change in parameters. Self-dualities put strong constraints on the structure of the phase diagram, especially at the self-dual critical point.

In this lecture note, we will discuss duality in the Topological Holography (TH) / Symmetry Topological Field Theory (symTFT) / Symmetry Topological Order (symTO) framework. The TH / symTFT / symTO framework provides a systematic way to discuss (some) duality. Moreover, using our recent study of sequential quantum circuits, we can make concrete statements about the relation of dual theories (what remains invariant and what can change). We start in section 2 with an introduction to the TH framework. In particular, we give the explicit example of realizing the 1+1D transverse field Ising model in a 'sandwich' structure with 2+1D topological order in the bulk. Then in section 3, we discuss how the Kramers-Wannier duality of the Ising chain can be induced by changing the top boundary condition of the sandwich. In section 4, we extend the discussion to the Kennedy-Tasaki transformation of the $1+1$D $\mathbb{Z}_2 \times \mathbb{Z}_2$ spin chain. We discuss using the sandwich construction how the four ground states in the SPT phase on an open chain maps to the four ground states in the symmetry breaking phase. We also discuss how the transformation allows us to map the critical theory at the symmetry breaking transition point to that at the transition between SPT phases. In section 5, we discuss a $2+1$D sandwich with $3+1$D $\mathbb{Z}_2$ topological order in the bulk and show how the gauging duality in the $2+1$D Ising theory is realized.

2 Topological Holography / Symmetry TFT / Symmetry TO

The TH / symTFT / symTO framework realizes a $d+1$D system as a 'sandwich' with a $(d+1)+1$D topological bulk and a gapped top boundary. Let's illustrate this with the simple example of a 1+1D sandwich with 2+1D Toric Code bulk which realizes the 1+1D spin chain with global $\mathbb{Z}_2$ symmetry.

In the next section, we are going to show how the Kramers-Wannier duality corresponds to changing the gapped boundary condition at the top while preserving all other parts of the sandwich.

A $1+1$D transverse field Ising model is defined on a spin 1/2 chain with Hamiltonian

$$\tilde{H} = -\sum_i \sigma_i^x - g\sum_i \sigma_i^z\sigma_{i+1}^z \tag{1}$$

The model has a global $\mathbb{Z}_2$ symmetry $\prod_i \sigma_i^x$. When $g << 1$, the model is in the symmetric phase; when $g >> 1$, the model is in the symmetry-breaking phase. The transition point is described by the 2D Ising CFT. Now we are going to write it in a more complicated form as a 'sandwich'. The advantage of this sandwich structure will show up when we discuss the Kramers-Wannier duality of the Ising chain.

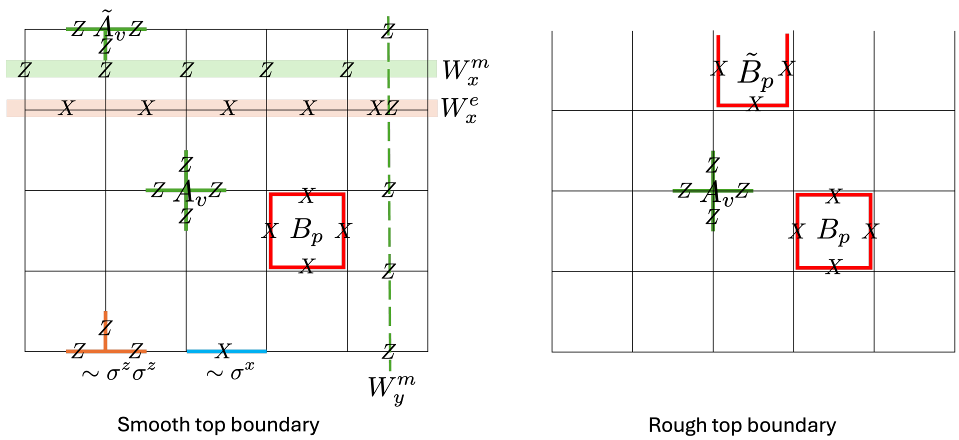

Figure 1: $1+1$D sandwich structure with $2+1$D Toric code in the bulk.

Consider the $2+1$D Toric Code on a square lattice with bulk Hamiltonian

$$H_{\text{TC}}^{\text{bulk}} = -\sum_v \left[\begin{array}{ccc} & Z & \\ Z & v & Z \\ & Z & \end{array} \right] - \sum_p \left[\begin{array}{ccc} & X & \\ X & \boxed{p} & X \\ & X & \end{array} \right], \tag{2}$$

With periodic boundary conditions, the logical operators that map between degenerate ground states are $W^e = \prod X$ and $W^m = \prod Z$ loop operators along nontrivial direct and dual lattice cycles, respectively. The superscript labels the e and m excitations created at the two ends of open string operators.

There are two possible gapped boundary conditions: a flux (m)-condensed boundary, called 'smooth', and a charge (e)-condensed boundary, called 'rough'. Concretely, the two boundaries correspond to ending the lattice on horizontal and vertical edges respectively and truncating the bulk Hamiltonian terms into three-body ones, as shown in Fig. 1 ($\tilde{A}_v$ and $\tilde{B}_p$). Consider the toric code model living on a cylinder (periodic boundary conditions in the horizontal direction) and fix the top boundary to be smooth or rough. When the cylinder is set to have finite size in the y direction but infinite size in the x direction, the sandwich becomes an effective $1+1$D system. The bulk and top boundary determine the low energy Hilbert space of the $1+1$D system. The bottom boundary is not fixed but left free, leaving dangling degrees of freedom in order to represent the dynamics of the effective $1+1$D model.

There are several kinds of operators in the formalism that each play a different role, as pictured in Fig. 1. First, there are the local stabilizers whose $+1$ eigenspace specifies the low-energy subspace in which the corresponding 1+1D theory is defined. These consist of all bulk stabilizers A_v and B_p, as defined in Eq. 2, and truncated vertex $\tilde{A}_v$ (for a smooth boundary) or plaquette $\tilde{B}_p$ (for a rough boundary) stabilizers at the top boundary. Next, the horizontal W_x^e and W_x^m string operators winding around the cylinder on the direct and dual lattice commute with all the bulk and top boundary stabilizers and act in the low-energy subspace. We will see that the ± 1 eigenvalue of W_x^e and W_x^m label different symmetry charge and symmetry flux sectors of the $1+1$D theory. Finally, there are two kinds of local operators at the bottom boundary—a single X and three Z's—that commute with all the aforementioned operators, and therefore act only within a given charge / flux sector of the low-energy subspace. These operators form a complete set of symmetric operators for each sector and determine the dynamics of the 1D theory.

Let us now match the Hilbert / operator space of the sandwich with that of the $1+1$D spin chain with global $\mathbb{Z}_2$ symmetry.

Consider first the case of a smooth top boundary (m-condensed). The horizontal W_x^m loop operator is equal to the product of $\tilde{B}_p$ stabilizers on the top boundary. Therefore, as long as there are no 'defects' on the top boundary, $W_x^m = 1$. (We will discuss in a minute the case where there is a defect on the top boundary and $W_x^m = -1$.) The W_x^e loop operator, on the other hand, is not fixed by the bulk and top boundary stabilizers and can take both ± 1 values. Therefore, W_x^e can be thought of as the $\mathbb{Z}_2$ global symmetry operator of the sandwich. The vertical W_y^m string operator anti-commutes with W_x^e and should be interpreted as the $\mathbb{Z}_2$ charge operator. Note that W_y^m does not create any excitation in the bulk or on the top boundary, and hence preserves the low-energy subspace of the $1+1$D system. When matched with operators in the $1+1$D Ising chain, we see that W_x^e becomes the $\prod \sigma^x$ symmetry operator and W_y^m becomes the σ^z charge operator. The three-body ZZZ operator on the bottom boundary is equivalent to the product of two W_y^m operators (next to each other) up to bulk and top boundary stabilizer terms. Therefore, it can be interpreted as the $\sigma^z\sigma^z$ Ising coupling term in the Ising chain. The single X operator on the bottom boundary anti-commutes with neighboring ZZZ terms and hence can be interpreted as the σ^x operator of the Ising chain.

$$\begin{aligned} \text{Smooth top Boundary :} & W_x^e \sim \prod \sigma^x, \ W_y^m \sim \sigma^z, \\ & \text{bottom boundary } ZZZ \sim \sigma^z\sigma^z, \ \text{bottom boundary } X \sim \sigma^x \end{aligned} \tag{3}$$

When we enforce that all X terms on the bottom boundary of the sandwich to have eigenvalue $+1$, this makes the bottom boundary a rough boundary. From the correspondence to the Ising chain, we see that with a smooth top boundary and a rough bottom boundary, the sandwich realizes the symmetric phase of the $\mathbb{Z}_2$ symmetry. Similarly, setting all ZZZ terms on the bottom boundary to be $+1$ creates a smooth bottom boundary and the whole sandwich is in the symmetry-breaking phase of the $\mathbb{Z}_2$ symmetry. In particular, when both top and bottom boundaries are smooth, applying the charge operator W_y^m does not create any excitation. Therefore, the symmetry charge is 'condensed' and the sandwich is in the symmetry-breaking phase.

Since W_x^e is the $\mathbb{Z}_2$ operator of the sandwich, its ± 1 eigenvalue labels the two charge sectors of the system. How to access the flux sector? We claim that the flux sector corresponds to the eigenvalue -1 sector of operator W_x^m. Because $W_x^m = \prod \tilde{B}_p$ on the top boundary, in this sector one of the $\tilde{B}_p$ terms on the top boundary has eigenvalue -1. This sector is orthogonal to the original one with $W_x^m = 1$. To see that this is the flux sector, let's find its mapping to the $1+1$D Ising chain. In the discussion above, we see that the sector with $W_x^m = 1$ has a mapping to the $1+1$D Ising chain with a direct correspondence of their operator algebra. To see how the $W_x^m = -1$ sector is related to the $1+1$D Ising chain, we can map it back to the $W_x^m = 1$ sector by applying W_y^e. W_y^e

commutes with the $\mathbb{Z}_2$ symmetry operator W_x^e, the $\mathbb{Z}_2$ charge operator W_y^m, the transverse field term of a single X on the bottom boundary and all but one of the Ising coupling term of ZZZ on the bottom boundary. Therefore, mapped to the Ising chain, it corresponds to the Hamiltonian

$$\tilde{H} = -\sum_i \sigma_i^x - g \sum_{i \neq N} \sigma_i^z \sigma_{i+1}^z + g\sigma_N^z \sigma_1^z \tag{4}$$

which is exactly the Hamiltonian of the Ising chain with a $\mathbb{Z}_2$ flux. Note that in the $1+1$D Ising chain, the different flux sectors correspond to models living in the same $2^{\otimes N}$-dimensional Hilbert space but with modified Hamiltonian (sign change at the boundary). In the sandwich construction, different flux sectors live in orthogonal Hilbert spaces while the dynamical terms on the bottom boundary are kept the same. The advantage of the sandwich construction is to treat charge sectors and flux sectors on equal footing (orthogonal sectors in a bigger Hilbert space while the Hamiltonian terms are kept invariant). This is a very helpful feature to have when discussing duality which maps between charge and flux sectors, as we see below. One thing that is lost in the process, though, is the tensor product structure of Hilbert space.

Therefore, the horizontal string operators $W_x^e = \pm 1$ and $W_x^m = \pm 1$ label the charge and flux sectors of the sandwich while the vertical W_y^m and W_y^e operators toggle between the sectors.

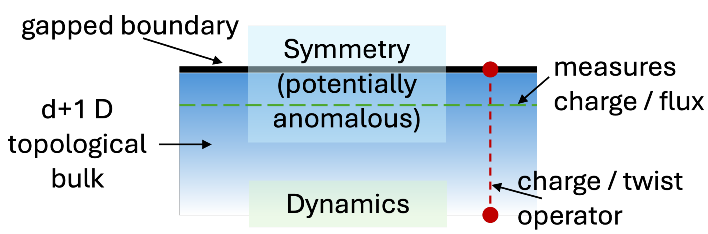

Figure 2: The sandwich structure in the Topological Holography framework.

This example illustrates the key features of the sandwich construction in the TH framework. As shown in Fig. 2, a $d+1$-dimensional sandwich

- has a $(d+1)+1$-dimensional (gapped) topological theory in the bulk,
- the top boundary is gapped by condensing certain topological excitations from the bulk,
- the bulk and top boundary Hamiltonian terms define the low-energy space of the sandwich,
- Hamiltonian terms on the bottom boundary generate the dynamics in the low-energy space,
- closed horizontal logical operators of the topological bulk parallel to the boundaries define the symmetry and flux sectors of the sandwich,
- open vertical logical operators connecting the top and bottom boundaries toggle between the sectors.

The sectors can be labeled by either the eigenvalues of the horizontal logical operators or the vertical logical operator that maps to each sector starting from the sector with positive eigenvalue for all horizontal logical operators. In a $1+1$D sandwich with a $2+1$D bulk, the second labeling is the anyon label.

In the example discussed, we have the simplest case where the symmetry is a conventional 0-form on-site $\mathbb{Z}_2$ symmetry. With different choices of the topological bulk, the sandwich can have more general forms of symmetries

- $2+1$D doubled-semion: the bulk contains a boson, a semion and their composite – an anti-semion. The top boundary can be gapped by condensing the boson. The symmetry of the sandwich is generated by the horizontal semion string operator, which generates an anomalous 0-form $\mathbb{Z}_2$ symmetry.
- $2+1$D doubled-Ising: the bulk anyon set is the composite of two chiral copies $(1,\psi,\sigma)\times(1,\bar{\psi},\bar{\sigma})$. The top boundary can be gapped by condensing both $\psi\bar{\psi}$ and $\sigma\bar{\sigma}$. The symmetry of the sandwich is generated by W_x^{ψ} and W_x^{σ} which satisfy the non-invertible fusion rule of $W_x^{\sigma}\times W_x^{\sigma}=1+W_x^{\psi}$.
- $3+1$D toric code: the bulk contains a bosonic point charge excitation and a flux loop excitation. The top boundary can be gapped by condensing the flux loop. In this case, the symmetry of the sandwich is generated by the string operators of the bosonic charge in the two directions parallel to the boundary. This corresponds to a 1-form $\mathbb{Z}_2$ symmetry in the $2+1$D sandwich.

3 Kramers-Wannier duality of $1+1$D Ising chain

The $1+1$D Ising model (a $+$ subscript is added to indicate that this is the model with no flux and periodic boundary condition)

$$\tilde{H}_+(g) = -\sum_i \sigma_i^x - g\sum_i \sigma_i^z\sigma_{i+1}^z \tag{5}$$

has a well-known self-duality. Under the duality, $\mathbb{Z}_2$ symmetric local operators map as

$$\sigma_i^x \to \sigma_i^z\sigma_{i+1}^z,\ \sigma_i^z\sigma_{i+1}^z \to \sigma_{i+1}^x \tag{6}$$

such that $\tilde{H}_+$ maps back to itself with a change of parameter $g\to 1/g$, $\tilde{H}_+(g)\to g\tilde{H}_+(1/g)$. The operator algebra (commutation relation) among the symmetric local operators is preserved, so this mapping works well locally. But globally it runs into the problem

$$\prod_i \sigma_i^x \to \prod_i \sigma_i^z\sigma_{i+1}^z = 1,\ 1 = \prod_i \sigma_i^z\sigma_{i+1}^z \to \prod_i \sigma_i^x \tag{7}$$

Therefore, the duality mapping works only in the no-charge (and no-flux) sector with $\prod_i \sigma_i^x$.

A slight modification of the duality mapping can be applied to other sectors. Consider the mapping

$$\sigma_i^z\sigma_{i+1}^z \to \sigma_{i+1}^x, \forall i,\ \sigma_i^x \to \sigma_i^z\sigma_{i+1}^z \text{ for } i\neq N,\ \sigma_N^x \to -\sigma_N^z\sigma_1^z, \tag{8}$$

The local operator algebra is still preserved while globally

$$\prod_i \sigma_i^x \to -\prod_i \sigma_i^z\sigma_{i+1}^z = -1,\ 1 = \prod_i \sigma_i^z\sigma_{i+1}^z \to \prod_i \sigma_i^x \tag{9}$$

The Hamiltonian $\tilde{H}_+$ is mapped to the twisted Hamiltonian with anti-periodic boundary condition

$$\tilde{H}_+(g) \to -\sum_{i\neq N}\sigma_i^z\sigma_{i+1}^z+\sigma_N^z\sigma_1^z-g\sum_i\sigma_i^x = g\left(-\sum_i\sigma_i^x - 1/g\sum_{i\neq N}\sigma_i^z\sigma_{i+1}^z+1/g\sigma_N^z\sigma_1^z\right) = g\tilde{H}_-(1/g) \tag{10}$$

Therefore, the charge-no-flux sector is mapped to the flux-no-charge sector under the duality mapping.

If we label the four sectors of the Ising chain as $(\pm1,\pm1)$ with the first ±1 labeling the charge / no-charge sector and the second ±1 labeling the flux / no-flux sector. Under duality, they are mapped as

$$(+1,+1)\leftrightarrow(+1,+1),\ (-1,+1)\leftrightarrow(+1,-1),\ (-1,-1)\leftrightarrow(-1,-1), \tag{11}$$

We can explicitly compare the low-energy spectrum in the symmetry-breaking phase and the symmetric phase (at the exactly solvable point) in the four sectors and see how they match before and after the duality mapping, as shown in Table 1.

	Symmetry breaking	Symmetric
Sector	$(1,1)$	$(1,1)$
GS	$\lvert\psi_{sb}\rangle = \lvert 00...0\rangle + \lvert 11...1\rangle$	$\lvert\psi_{sym}\rangle = \lvert ++...+\rangle$
Ex.	$\prod_{i_0}^{i_1} X_i \lvert\psi_{sb}\rangle$	$Z_{i_0}Z_{i_1}\lvert\psi_{sym}\rangle$
Sector	$(1,-1)$	$(-1,1)$
GS	$\prod_{i_0}^{N} X_i \lvert\psi_{sb}\rangle$	$Z_{i_0}\lvert\psi_{sym}\rangle$
Ex.	$\prod_{i_1}^{i_2} X_i \prod_{i_0}^{N} X_j \lvert\psi_{sb}\rangle$	$Z_{i_0}Z_{i_1}Z_{i_2}\lvert\psi_{sym}\rangle$
Sector	$(-1,1)$	$(-1,1)$
GS	$\lvert\psi_{sb}\rangle' = \lvert 00...0\rangle - \lvert 11...1\rangle$	$\lvert\psi_{sym}\rangle$
Ex.	$\prod_{i_0}^{i_1} X_i \lvert\psi_{sb}\rangle$	$Z_{i_0}Z_{i_1}\lvert\psi_{sym}\rangle$
Sector	$(-1,-1)$	$(-1,-1)$
GS	$\prod_{i_0}^{N} X_i \lvert\psi_{sb}\rangle'$	$Z_{i_0}\lvert\psi_{sym}\rangle$
Ex.	$\prod_{i_1}^{i_2} X_i \prod_{i_0}^{N} X_j \lvert\psi_{sb}\rangle'$	$Z_{i_0}Z_{i_1}Z_{i_2}\lvert\psi_{sym}\rangle$

Table 1: Spectrum matching. We list ground states and 1st excited states within each sector

When the Ising chain is realized as a 1+1D sandwich as discussed above, the duality transformation corresponds to changing the top boundary from smooth to rough (and vice verse). We discussed the case of smooth top boundary above. Let's now consider the case of rough top boundary, as shown in Fig. 3. The case of smooth boundary is also shown for comparison. The discussion is completely analogous to the one for smooth boundary and we will see explicitly how duality is induced once the boundary type is changed.

A rough top boundary ends on vertical edges and the bulk Hamiltonian terms B_p are truncated into three-body ones $\tilde{B}_p$. The e anyons are condensed on the rough boundary because a W_y^e string can end on the rough boundary without leaving any excitation. The horizontal W_x^e operator is fixed by the boundary while the horizontal W_x^m operator is now the $\mathbb{Z}_2$ symmetry operator of the sandwich. The sandwich therefore still represents a $1+1$D system with global (non-anomalous) $\mathbb{Z}_2$ symmetry – the Ising chain. Therefore the duality induced by the change from smooth to rough boundary is a self-duality. The W_y^e operator is now the symmetry charge operator since it anti-commutes with W_x^m. The single X term on the bottom boundary is equal to the product of two W_y^e operators next to each other. Therefore, it is identified with the Ising coupling term $\sigma_i^z\sigma_{i+1}^z$ in the Ising chain. The ZZZ operator on the boundary is now identified with the transverse field term σ^x which is

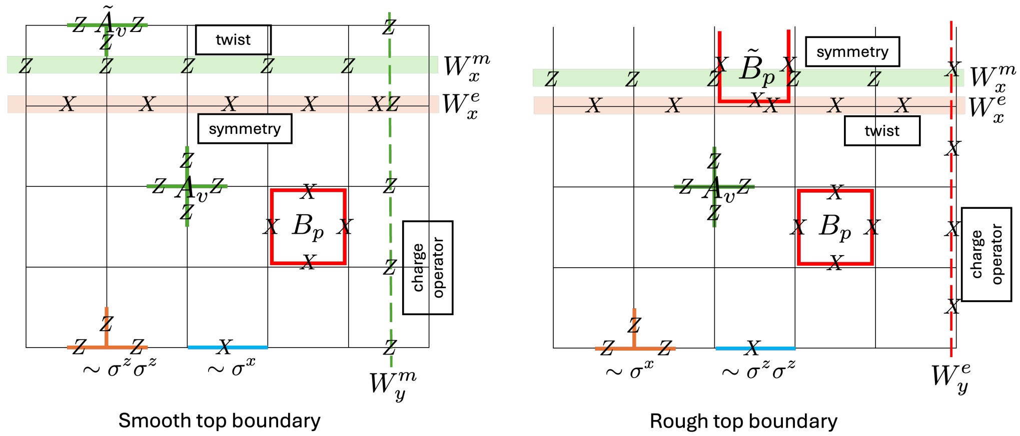

Figure 3: $1+1$D sandwich structure with $2+1$D Toric code in the bulk.

consistent with the fact that the product of all such operators along the boundary gives the $\mathbb{Z}_2$ symmetry operator W_x^m. The operator correspondence can be summarized as follows:

$$\text{Rough top Boundary} : W_x^m \sim \prod \sigma^x,\ W_y^e \sim \sigma^z,$$
$$\text{bottom boundary } X \sim \sigma^z\sigma^z,\ \text{bottom boundary } ZZZ \sim \sigma^x \tag{12}$$

Comparing this to Eq. 3, we see that when the top boundary is changed from smooth to rough, the interpretation of bottom boundary operators in terms of symmetric operators in the Ising chain is exactly the opposite. We want to emphasize that, when the boundary type changes, the Hamiltonian terms on the bottom boundary do not change. It is their interpretation as Ising chain operators that change. Moreover, the role of W_x^e and W_x^m are also switched. With smooth boundary, W_x^e measures symmetry charge while W_x^m measures symmetry flux; with rough boundary, W_x^m measures symmetry charge while W_x^e measures symmetry flux. When the boundary type changes, W_x^e and W_x^m do not change as they live in the bulk. Again it is their interpretation as charge and flux sector labels that change. Note that the boundary change automatically takes care of the mapping in different sectors, as given in for example Eq. 6 and 8. To see this, we notice that the bottom boundary Hamiltonian terms do not change in the process, but their interpretation as Ising chain operator changes. As discussed above, with fixed top boundary, in the flux sector, one of the bottom boundary terms that correspond to the Ising coupling term get a minus sign when mapped to the Ising coupling term, as discussed around Eq. 4. With this extra minus sign, the induced duality mapping exactly matches with that given in Eq. 6 and 8.

From this discussion, we see that duality mapping in the symmetry TFT / Topological holography framework corresponds to changing the gapped top boundary condition in the sandwich without touching the bulk or the bottom boundary. Therefore, the bulk operators and bottom boundary operators do not change, but their interpretation may change due to the change in the top boundary condition. We can further show that the change in top boundary condition can be induced by a unitary quantum circuit applied to the top boundary only. The unitarity of the circuit is the reason that the spectrum before and after the duality mapping are exactly the same in corresponding sectors, as shown in Table 1. This is a generic feature for dualities in the symmetry TFT / topological holography framework.

The circuit that maps from the rough to the smooth boundary is illustrated in Fig. 4. Let's look at what the circuit does to the stabilizers when going from a rough to a smooth boundary. Starting from the rough boundary, all truncated plaquette terms $\tilde{B}_p$ have eigenvalue $+1$ except for the one

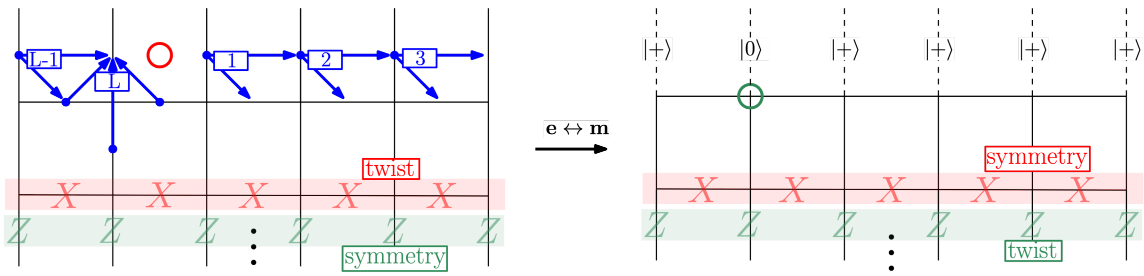

Figure 4: Kramers-Wannier duality via unitary sequential quantum circuit in the toric code sandwich going from rough to smooth boundary. After the circuit, we are left with a smooth boundary with an omitted boundary stabilizer at the position marked by the hollow circle, and all rough legs are disentangled into product states. After the circuit, the eigenvalues of the bulk symmetry and twist operators remain unchanged, but their roles are reversed.

at the red circle which has eigenvalue $+1$ in the no flux sector and -1 in the flux sector. On the resulting smooth boundary, all truncated vertex terms $\tilde{A}_v$ have eigenvalue $+1$ except for the one at the green circle which has eigenvalue $+1$ in the new no flux sector and -1 in the new flux sector.

Under the circuit, the boundary plaquette terms and bulk vertex terms near the boundary (except the circled ones) are mapped as follows:

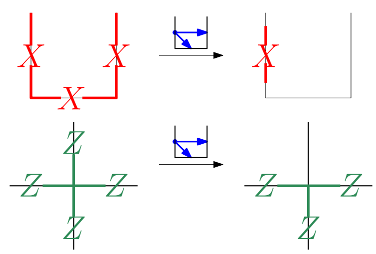

(13)

where the controlled-NOT gates are centered on the top-right plaquette in the lower expression. The $\tilde{B}_p$ term at the red circle is mapped to the W_x^e string operator which is consistent with the fact that with rough boundary, the two have the same eigenvalue. The vertex term at the green circle is mapped as,

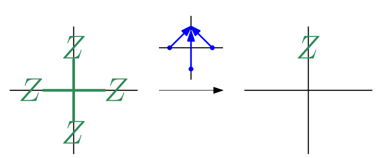

(14)

The truncated $\tilde{A}_v$ term at the green circle on the smooth boundary is mapped from the W_x^m string operator, which is also consistent with the fact that with smooth boundary, they have the same eigenvalue.We see that the rough edges get disentangled from the bulk by the circuit, and that the new boundary stabilizers are that of the smooth boundary. Since the horizontal string operators in the bulk are not touched by the circuit, their eigenvalues remain unchanged, as claimed in the previous section. A similar circuit can be constructed to map from the smooth to the rough boundary.

4 Kennedy-Tasaki duality of $1+1$D $\mathbb{Z}_2 \times \mathbb{Z}_2$ spin chain

We have discussed the Kramers-Wannier duality in the Ising chain in great detail. The Kramers-Wannier duality is special in that there are only two gapped phases in the phase diagram which map into each other and the critical point in between is self-dual. In this section, we are going to discuss the Kennedy-Tasaki duality in a $\mathbb{Z}_2 \times \mathbb{Z}_2$ symmetric spin chain using the sandwich construction. The Kennedy-Tasaki duality was originally designed to map the nontrivial SPT phase to the symmetry-breaking phase. It is also a self-duality in the sense that the system before and after the duality mapping are both $1+1$D spin chains with $\mathbb{Z}_2 \times \mathbb{Z}_2$ symmetry. But this is a more general case than Kramers-Wannier. There are six gapped phases in the $1+1$D spin chains with $\mathbb{Z}_2 \times \mathbb{Z}_2$ symmetry. The duality induces a permutation among the six phases and the phase transitions in between. We are going to use the sandwich construction to see how Kennedy-Tasaki permutes the full phase diagram and relates different phase transitions to each other.

Consider a $1+1$D spin chain with two sets of $\mathbb{Z}_2$ degrees of freedom, σ and τ, located on odd and even sites respectively. The system has a $\mathbb{Z}_2 \times \mathbb{Z}_2$ symmetry generated by $\prod_i \sigma^x_{2i-1}$ and $\prod_i \tau^x_{2i}$. The trivial symmetric phase is realized with the Hamiltonian

$$H_{\mathrm{SPT}_0} = -\sum_i \sigma^x_{2i-1} - \sum_i \tau^x_{2i} \tag{15}$$

The fully symmetry-breaking phase is realized with the Hamiltonian

$$H_{\mathrm{SB}} = -\sum_i \sigma^z_{2i-1}\sigma^z_{2i+1} - \sum_i \tau^z_{2i}\tau^z_{2i+2} \tag{16}$$

The nontrivial SPT phase is realized with the Hamiltonian

$$H_{\mathrm{SPT}_1} = -\sum_i \tau^z_{2i-2}\sigma^x_{2i-1}\tau^z_{2i} - \sum_i \sigma^z_{2i-1}\tau^x_{2i}\sigma^z_{2i+1} \tag{17}$$

With the open boundary condition, the nontrivial SPT phase has a four-fold ground state degeneracy, two-fold on each edge. The edge states can be recoupled back with boundary terms $\pm\tau^z_{2N}\sigma^x_1\tau^z_2$ and $\pm\sigma^z_{2N-1}\tau^x_{2N}\sigma^z_1$. The four boundary terms correspond to the four different flux sectors on a closed chain and the ground states in these four sectors carry different charges. In particular, a τ flux carries a σ charge and a σ flux carries a τ charge. The Kennedy-Tasaki transformation maps these four ground states of the nontrivial SPT phase to the four-fold ground states of the symmetry-breaking phase.

Now let's see how this mapping is realized in a sandwich structure by changing top boundary conditions. Consider a $1+1$D sandwich with the $2+1$D $\mathbb{Z}_2 \times \mathbb{Z}_2$ topological order in the bulk (i.e. two copies of Toric Code). There are 16 anyons in the bulk $(1, e_1, m_1, \psi_1) \times (1, e_2, m_2, \psi_2)$. There are six types of gapped boundaries corresponding to the condensation of

$$\begin{aligned} &\mathcal{A}_1 : \{1, e_1, e_2, e_1e_2\}, && \mathcal{A}_2 : \{1, e_1, m_2, e_1m_2\}, && \mathcal{A}_3 : \{1, m_1, e_2, m_1e_2\} \\ &\mathcal{A}_4 : \{1, e_1e_2, m_1m_2, \psi_1\psi_2\}, && \mathcal{A}_5 : \{1, m_1, m_2, m_1m_2\}, && \mathcal{A}_6 : \{1, m_1e_2, e_1m_2, \psi_1\psi_2\} \end{aligned} \tag{18}$$

We are going to focus on the duality transformation induced by changing from boundary $\mathcal{A}_1$ to $\mathcal{A}_6$. In Table 4, we list the gapped phases realized in the sandwich with top boundary $\mathcal{A}_1$ and $\mathcal{A}_6$ and the bottom boundary in one of the six gapped states. The symmetry-breaking pattern of the gapped phases can be deduced from the set of anyons that can tunnel between the two boundaries without creating excitations on either boundary.

	$\mathcal{A}_1$	$\mathcal{A}_2$	$\mathcal{A}_3$	$\mathcal{A}_4$	$\mathcal{A}_5$	$\mathcal{A}_6$
$\mathcal{A}_1$	SSB $\to 1$	SSB $\to \mathbb{Z}_2$	SSB $\to \mathbb{Z}_2$	SSB $\to \mathbb{Z}_2$	SPT_0	SPT_1
$\mathcal{A}_6$	SPT	SSB $\to \mathbb{Z}_2$	SSB $\to \mathbb{Z}_2$	SSB $\to \mathbb{Z}_2$	SPT	SSB $\to 1$

From the last column in the table, we see that changing from the $\mathcal{A}_1$ top boundary to the $\mathcal{A}_6$ top boundary induces a duality mapping from the nontrivial SPT phase (the Haldane phase) to the fully symmetry-breaking phase, which is exactly the effect of Kennedy-Tasaki. (From the first column, we see that the same duality takes the fully symmetry-breaking phase to a symmetric phase, although with the $\mathcal{A}_6$ top boundary, it is ambiguous to say whether it is a trivial or nontrivial SPT.) Following a similar analysis as in the previous section, we can identify the corresponding sectors and match their spectrum before and after the mapping. In particular, we can see how the four-fold degenerate edge states of the nontrivial SPT on an open chain map to the four-fold degenerate ground state in the fully symmetry-breaking phase.

With the $\mathcal{A}_1$ top boundary, the sandwich has $\mathbb{Z}_2 \times \mathbb{Z}_2$ symmetry generated by $W_x^{m_1}$ and $W_x^{m_2}$. The flux sectors are labeled by the eigenvalues of $W_x^{e_1}$ and $W_x^{e_2}$. With the $\mathcal{A}_6$ top boundary, the flux sectors are labeled by the eigenvalues of $W_x^{m_1 e_2}$ and $W_x^{e_1 m_2}$. The $\mathbb{Z}_2 \times \mathbb{Z}_2$ symmetry is generated by $W_x^{m_1}$ and $W_x^{m_2}$, or equivalently by $W_x^{e_1}$ and $W_x^{e_2}$. From the above discussion we see that the four-fold degenerate edge states of the SPT correspond to the four flux sectors of the spin chain and each flux is attached to corresponding charges. In the sandwich structure, with $\mathcal{A}_1$ top boundary top boundary and $\mathcal{A}_6$ bottom boundary, these four ground states are ground states in the $\{W_x^{m_1} = 1, W_x^{m_2} = 1, W_x^{e_1} = 1, W_x^{e_2} = 1\}$, $\{W_x^{m_1} = -1, W_x^{m_2} = 1, W_x^{e_1} = 1, W_x^{e_2} = -1\}$, $\{W_x^{m_1} = 1, W_x^{m_2} = -1, W_x^{e_1} = -1, W_x^{e_2} = 1\}$, $\{W_x^{m_1} = -1, W_x^{m_2} = -1, W_x^{e_1} = -1, W_x^{e_2} = -1\}$ sectors respectively. When the top boundary is changed from $\mathcal{A}_1$ to $\mathcal{A}_6$, the ground states in these sectors remain the lowest energy, although the interpretation of $W_x^{m_1}$, $W_x^{m_2}$, $W_x^{e_1}$ and $W_x^{e_2}$ changes. Since with $\mathcal{A}_6$ top boundary, $W_x^{m_1}$ and $W_x^{m_2}$ (or equivalently $W_x^{e_2}$ and $W_x^{e_1}$) measures the $\mathbb{Z}_2 \times \mathbb{Z}_2$ symmetry charges, the four ground states after the duality transformation carries different symmetry charges but the same symmetry flux – they are the degenerate ground states of the symmetry breaking phase.

More interestingly, we can learn about the critical point at phase transitions using the duality map. Consider the first column and the fifth column. We see that the KT duality maps the symmetry-breaking transition (from fully symmetric trivial SPT phase to fully symmetry-breaking phase) to the transition between the two SPTs. The symmetry-breaking transition is very well understood – it is two copies of the Ising CFT, one for each $\mathbb{Z}_2$. The duality tells us that there is a continuous transition between the trivial and nontrivial SPT and the critical theory is basically also two copies of Ising CFT. The possible difference between the two critical theories is the reorganization of different symmetry sectors. Let's take what is known about the Ising CFT and find out about the critical theory between the two $\mathbb{Z}_2 \times \mathbb{Z}_2$ SPTs.

A single Ising CFT contains four sectors: the trivial sector labeled $++$, the charge sector labeled $-+$, the flux sector labeled $+-$ and the fermion sector (composite of charge and flux) $--$. Each sector contains several primary fields and their descendants. The partition function of each sector is a sum over the conformal towers associated with the contained primary fields.

$$Z_{++}^{\text{Ising}} = Z_1 + Z_\epsilon,\ Z_{-+}^{\text{Ising}} = Z_\sigma,\ Z_{+-}^{\text{Ising}} = Z_\mu,\ Z_{--}^{\text{Ising}} = Z_\phi + Z_{\bar{\phi}} \tag{19}$$

1 is the trivial primary field, ϵ is the energy primary field, σ is the spin (order parameter) primary field, μ is the disorder parameter primary field, ϕ and $\bar{\phi}$ are the left and right moving fermions. The spectrum of the Ising model in Eq. 1 contains only the charge sectors. Therefore the total partition function is

$$Z^{\text{Ising}} = Z_{++}^{\text{Ising}} + Z_{-+}^{\text{Ising}} = Z_1 + Z_\epsilon + Z_\sigma \tag{20}$$

This is the well-known partition function of Ising CFT. We can also understand this combination of sectors in the total partition function from the sandwich structure discussed in the previous section. In the sandwich with a single copy of Toric Code in the bulk, suppose that the top boundary is gapped with the condensation of the e anyon. Only the two charge sectors are contained in the sandwich without any defect on the top boundary. Therefore, the top boundary chooses the two charge sectors when forming the $1+1$D sandwich and $Z^{\text{Ising}}_{tot} = Z^{\text{Ising}}_{++} + Z^{\text{Ising}}_{-+}$.

The symmetry-breaking transition in a $\mathbb{Z}_2 \times \mathbb{Z}_2$ spin chain is simply two copies of the Ising CFT.

$$Z^{\text{Ising}^2} = (Z_1 + Z_{\epsilon_1} + Z_{\sigma_1})\,(Z_1 + Z_{\epsilon_2} + Z_{\sigma_2}) \tag{21}$$

which contains the four charge sectors of the $\mathbb{Z}_2 \times \mathbb{Z}_2$ spin chain

$$Z^{\text{Ising}^2} = Z^{\text{Ising}^2}_{++,++} + Z^{\text{Ising}^2}_{++,-+} + Z^{\text{Ising}^2}_{-+,++} + Z^{\text{Ising}^2}_{-+,-+} \tag{22}$$

This can again be understood from the perspective of the sandwich structure. The symmetry-breaking transition is realized in the $\mathbb{Z}_2 \times \mathbb{Z}_2$ sandwich with top boundary being $\mathcal{A}_1$ and the bottom boundary between $\mathcal{A}_1$ and $\mathcal{A}_5$. The four charge sectors in the partition function is chosen by the $\mathcal{A}_1$ top boundary where $\{1, e_1, e_2, e_1e_2\}$ condense.

Now if we change the top boundary to $\mathcal{A}_6$, the condensate changes to $\{1, e_1m_2, m_1e_2, \psi_1\psi_2\}$. Therefore, the sectors that show up at the critical point are

$$Z^{\text{SPT}\to\text{SPT}} = Z^{\text{Ising}^2}_{++,++} + Z^{\text{Ising}^2}_{-+,+-} + Z^{\text{Ising}^2}_{+-,-+} + Z^{\text{Ising}^2}_{--,--} \tag{23}$$

which in terms of the single Ising conformal towers takes the form

$$Z^{\text{SPT}\to\text{SPT}} = (Z_1 + Z_{\epsilon_1})(Z_1 + Z_{\epsilon_2}) + Z_{\sigma_1}Z_{\mu_2} + Z_{\mu_1}Z_{\sigma_2} + (Z_{\phi_1} + Z_{\bar{\phi}_1})(Z_{\phi_2} + Z_{\bar{\phi}_2}) \tag{24}$$

5 Gauging of $2+1$D Ising model

Finally, let's consider a $2+1$D sandwich with a $3+1$D topological order in the bulk. Let's consider the simplest case of the $3+1$D toric code in the bulk. The sandwich can realize a $2+1$D spin system with either a 0-form $\mathbb{Z}_2$ symmetry or a 1-form $\mathbb{Z}_2$ symmetry. As we will see, the duality induced corresponds to the one between the $2+1$D Ising model and the $2+1$D $\mathbb{Z}_2$ gauge theory.

The $3+1$D toric code can be realized on 3D cubic lattice with Hamiltonian

$H^{\text{bulk}}_{\text{3DTC}} = -\sum_v \Big[$ 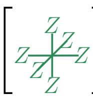 $\Big] - \sum_{p,xz} \Big[$ 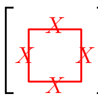 $\Big]$

$- \sum_{p,yz} \Big[$ 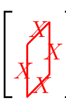 $\Big] - \sum_{p,zy} \Big[$ 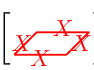 $\Big]$, (25)

with the plaquettes living in the three planes according to Fig. **??**. The bulk topological phase hosts two types of excitations: point-like charge (e) excitations that live on the endpoints of X-strings and string-like flux-loop excitations (m) that live at the boundary of membranes formed by Z-operators on the dual lattice. We will focus on two possible types of top boundary usually called 'rough' and 'smooth' (in analogy with the 2D case). At the 'rough' boundary, the lattice terminates on vertical edges and the vertical plaquette terms near the boundary are truncated into three-body $\tilde{B}_p$ terms. At the 'smooth' boundary, the lattice terminates on horizontal plaquettes, and the vertex terms near the boundary are truncated into five-body $\tilde{A}_v$ terms.

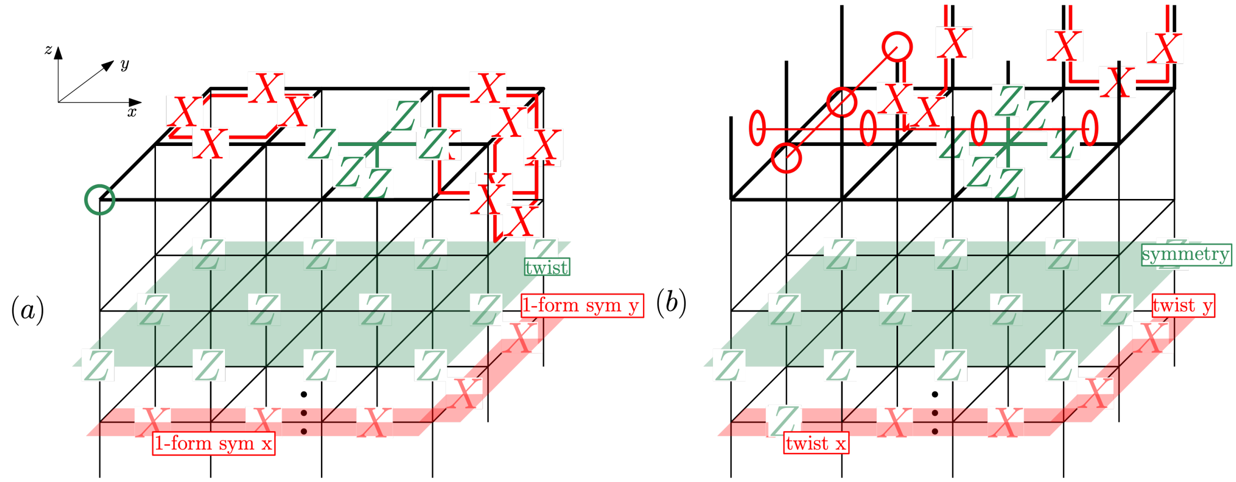

Figure 5: 3D toric code in the sandwich picture with smooth top boundary (a) and rough top boundary (b). Boundaries in the x and y direction are periodic. The unshaded terms are the boundary stabilizers (enforced) and the eigenvalues of the shaded terms label the symmetry or twist sectors depending on the top boundary. The hollow circles denote the location of omitted boundary stabilizers. For visual clarity, we have not drawn the operators $\mathcal{X}_z$, $\mathcal{Z}_{xz}$, or $\mathcal{Z}_{yx}$ which toggle between the sectors of the Hilbert space.

The bulk and top boundary terms define the low-energy sub-space of the sandwich. Logical operators parallel to the boundaries label the symmetry and flux sectors. These include the membrane operator V^m_{xy} and string operators W^e_x, W^e_y. With the rough top boundary, W^e_x, W^e_y are determined by the top boundary while V^m_{xy} is not. Therefore, V^m_{xy} becomes the 0-form $\mathbb{Z}_2$ symmetry of the sandwich while W^e_x, W^e_y measures the $\mathbb{Z}_2$ flux in the x and y directions respectively. On the other hand, with the smooth top boundary, V^m_{xy} is determined by the top boundary while W^e_x, W^e_y are not. Therefore, the sandwich has a 1-form $\mathbb{Z}_2$ symmetry with symmetry operators along nontrivial cycles being W^e_x, W^e_y. V^m_{xy} then measures the flux of the 1-form symmetry.

Table 5 lists gapped phases realized by the $2+1$D sandwich with smooth / rough top boundary and smooth / rough bottom boundary respectively. We see that, when the top boundary is changed from rough to smooth, a (0-form) $\mathbb{Z}_2$ symmetric phase is mapped to the $\mathbb{Z}_2$ gauge theory while the 0-form symmetry breaking phase is mapped to a trivial phase. This is exactly the gauging map for the phases in for $2+1$D Ising system.

	symmetry	bottom smooth	bottom rough
top smooth	1-form $\mathbb{Z}_2$	$\mathbb{Z}_2$ gauge theory (1-form SB)	trivial 1-form symmetric phase
top rough	0-form $\mathbb{Z}_2$	trivial 0-form symmetric phase	Ising ferromagnet (0-form SB)